ACS APPLIED MATERIALS & INTERFACES

Research Article

www.acsami.org

Controlling Nanostructures by Templated Templates: Inheriting Molecular Orientation in Binary Heterostructures

Tobias Breuer* and Gregor Witte

Fachbereich Physik, Philipps-Universität Marburg, 35032 Marburg, Germany

Supporting Information

ABSTRACT: Precise preparation strategies are required to fabricate molecular nanostructures of specific arrangement. In bottom-up approaches, where nanostructures are gradually formed by piecing together individual parts to the final structure, the self-ordering mechanisms of the involved structures are utilized. In order to achieve the desired structures regarding morphology, grain size, and orientation of the individual moieties, templates can be applied, which influence the formation process of subsequent structures. However, this strategy is of limited use for complex architectures because the templates only influence the structure formation at the interface between the template and the first compound. Here, we discuss the implementation of so-called templated templates and analyze to what extent orientations of the initial layers are inherited in the top layers of another compound to enable structural control in binary heterostructures. For that purpose, we prepared crystalline templates of the organic semiconductors pentacene and perfluoropentacene in different exclusive orientations. We observe that for templates of both individual materials the molecular orientation is inherited in the top layers of the respective counterpart. This behavior is also observed for various other molecules, indicating the robustness of this approach.

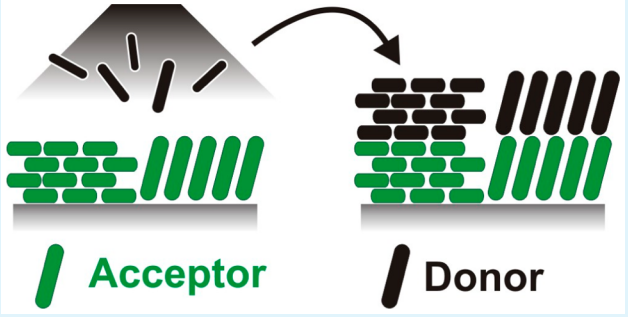

KEYWORDS: *organic semiconductors, organic heterostructures, pentacene, NEXAFS, atomic force microscopy, interfaces*

1. INTRODUCTION

Understanding the mechanisms of molecular assembly and structure formation is of key importance for the realization of novel artificial structures. One particular approach is templating, which occurs in nature on various length scales. For example, natural or artificial trellises are used to enable alignment and structuring of macroscopic plant growth, while biocompatible templates even allow one to steer the formation process of organic and inorganic adlayers ranging from mesoscopic to microscopic scales. Moreover, DNA templates can be used to build nanostructures of organic and inorganic materials.[1,2] Also imprints of biocells are applied to manipulate the shape and molecular characteristics of different stem cells.[3] Other examples are patterned arrays of proteins, which enable control of the nucleation sites, particle size, and shape as well as crystallographic orientation of natural biominerals,[4,5] as utilized in the bone growth or formation of sea shells.[6] These examples have inspired novel structuring methods to create artificial nanostructures by piecing together individual molecular entities to the final structure (*bottom-up* approach).

In a surface science approach, single-crystalline substrates are used as templates to control the adsorption structure of molecular films. Spontaneous ordering mechanisms are found such as self-assembly[7,8] and supramolecular architectures,[9,10] which result from covalent intermolecular coupling and chemisorption at the substrate surface. Although these mechanisms allow one to construct sophisticated two-dimensional structures especially on single-crystalline metal surfaces,[11,12] they cannot be directly applied to construct three-dimensional objects. Instead, the structural precision is lost upon the deposition of additional material, and further growth is found to be decoupled from the initial seeding layer because the growth is mostly governed by the crystalline structure and surface free energy of the adlayer material.[13] One possible alternative allowing for the preparation of three-dimensional objects are metal−organic frameworks.[14] Utilizing covalent linkers between different metal−organic entities, complex structures can be built. With the aid of appropriate anchor groups, these frameworks can also be attached to surfaces, yielding so-called surface-attached metal−organic framework (SURMOF) multilayers.[15−17]

Unfortunately, most of these strategies cannot be applied to van-der-Waals-bound solids like organic semiconductor (OSC) films because they are based on covalent coupling mechanisms. Because their optoelectronic characteristics are highly anisotropic, structural control over OSC thin films is an important challenge for the fundamental study and realization of organic electronic devices.[18−21] Therefore, appropriate strategies are required to gain structural control in these systems. Some recent reports indicate that templates with rather weak coupling

Received: August 11, 2015
Accepted: August 25, 2015
Published: August 25, 2015

DOI: 10.1021/acsami.5b07409
ACS Appl. Mater. Interfaces 2015, 7, 20485−20492

are promising in this context: using lattice matching between substrate and adsorbate (e.g., graphite or alkali halide surfaces) allows control of the molecular orientation and alignment in the initial layer.[22−24] Because the rather weak binding situation of the molecules on such inert surfaces allows for a slight molecular reorientation, the relaxed interface structures become compatible with packing motifs in the bulk structures, which results in homogeneous, rather extended crystallites with the desired molecular orientation.[22,25] This is strongly advantageous compared to thin films grown on metal surfaces. Although upon deposition on metal surfaces planar π-conjugated molecules almost exclusively adsorb in lying orientations in the first layer, this arrangement is frequently lost in further molecular layers and changes to upright orientations.[26−28]

However, using weakly interacting substrates does not directly provide structural control over stacked binary heterostructures because growth of the subsequently processed moieties is decoupled from the supporting substrate. Furthermore, common templates can only be used to achieve one specific final structure. Besides strategies, where the quality of the supporting substrate is intentionally lowered to obviate a template effect,[22,25] it is not possible to independently control the molecular and crystalline orientation on top of the template. These are undesirable limitations because the optoelectronic properties in multinary organic films like energy, diffusion, and decay dynamics of charge-transfer excitons depend decisively on the mutual orientation of the molecules as well as the crystalline order in such films.[29−31] Moreover, the microscopic characterization and experimental examination of the present theoretical models of elementary charge-transfer processes and exciton dynamics at internal interfaces are largely hampered by the ill-defined nature of such interfaces in real devices.[32] Therefore, efficient alternative structuring strategies are required for these materials. This is especially important because top-down structuring methods like lithography cannot be applied to organic films.

Here, we report on the detailed investigation of a different strategy to gain structural control even in complex systems such as binary molecular heterostructures: if the bottom layer features high structural order and sufficient molecular anisotropy, the bottom layer can also act as a template for the top layer. Controlling the molecular and crystalline orientation in the bottom layer will then allow one to also direct the final structure of the second compound even in thick multilayer films. In selected cases, this approach has been proven successful, e.g., in molecular combinations of *p*-sexiphenylene (*p*-6P, $C_{36}H_{26}$) and α-sexithiophene (6T, $C_{24}H_{14}S_6$)[33,34] as well as 3,4,9,10-perylenetetracarboxylic dianhydride (PTCDA) and copper phthalocyanine (CuPc)[35] or CuPc/F16-CuPc heterostructures.[36] Also, for the combination of the OSC pentacene (PEN, $C_{22}H_{14}$) and perfluoropentacene (PFP, $C_{22}F_{14}$), indications are found that upright molecular orientations can be inherited in the top layers.[37−39] However, a number of important points typically have not been addressed sufficiently in these previous studies:

(i) In subsequently processed heteroorganic stacks with two compounds and two distinctly different molecular orientations (upright and lying configurations), at least four different stack formations must be examined (both molecular orientations in the bottom layer for both compounds). Most importantly, structural inheritance can only be reasoned if for all mutual configurations the orientation of the bottom layer is inherited in the top layers. This constitutes an important difference from cases where coincidentally top-layer orientations similar to those in the bottom layer are observed as result of the respective surface free energies. This is, e.g., the case for CuPc/PTCDA combinations, where lying molecular orientations of PTCDA are observed on CuPc bottom layers in both, upright and lying orientations. In such cases, one can hardly argue that the bottom layer has controlled the growth mode of the top-layer compound, but instead these films grow equivalently to molecules on bare, weakly interacting substrates.

(ii) Although in molecular bilayer systems the molecular orientation of the bottom layer is adopted in many cases,[40−42] this structural precision is frequently lost in higher film thicknesses. Therefore, the molecular orientation in such heterostructures has to be precisely analyzed in different thickness regimes of both compounds, requiring a comprehensive study. In particular, this can only be achieved by combining appropriate methods enabling different probe depths.

(iii) In the previous studies, only the molecular orientation is controlled, but no evidence for polymorphism control mediated by the bottom layers has been reported.

In this work, we present a detailed study in which all of these aspects are appropriately addressed by comparing all possible mutual configurations of PEN and PFP directly at the interface and in bulklike multilayer films. The combination of these two OSCs serves as an important model system for organic donor/acceptor pairs and has already been used for the fabrication of ambipolar organic field-effect transistors.[43] By variation of the supporting substrate for the bottom layer, the initial orientation and crystal polymorph of the templating bottom layer can be precisely controlled,[22−24,44−47] allowing the preparation of all aforementioned different stack combinations. This has enabled us to study the templating effect of different molecular orientations and also of different polymorphs in the template for both materials. In particular, we directly observe polymorphism control in the top layer mediated by the bottom layer. Furthermore, the concept of structural inheritance has been additionally qualified in this work by analyzing complementary heterostructures of PFP with *p*-6P as well as 5,7,12,14-pentacenetetrone (P-TET).

To gain insight into the surface of the processed stacks, as well as the molecular orientation in thick layers and at the internal interface, experimental methods with different probe depths have been combined (cf. Figure 1b): atomic force microscopy (AFM) was used to analyze the surface and

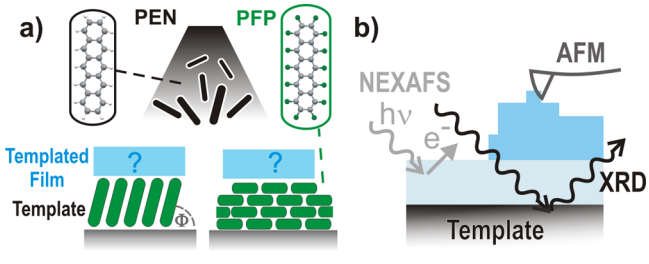

Figure 1. (a) Schemes of different molecular templates depicted for the case of PFP (green) with subsequent deposition of PEN (black), explaining the symbols and color code used in all figures. (b) Summary of the utilized characterization methods showing different probe depths (color code: template, black; interface layer, light blue; templated multilayer, dark blue).

DOI: 10.1021/acsami.5b07409
ACS Appl. Mater. Interfaces 2015, 7, 20485−20492

morphology of the templates and templated films without providing information from deeper layers. X-ray diffraction (XRD), by contrast, is sensitive to the crystalline order in the complete sample, i.e., in top layers as well as bottom layers in comparably thick samples (typically 30 nm thickness of both compounds). To exclusively determine the orientation at the interface between both compounds, synchrotron-based near-edge X-ray absorption fine-structure spectroscopy (NEXAFS) has been applied to samples in the initial stage of growth of the top-layer compound (nominal thickness 2 nm). Because of its low probe depth (~2 nm), this technique is highly surface-sensitive, hence allowing one to derive the effective molecular orientation ϕ (cf. Figure 1) directly at the interface even in noncrystalline configurations.[48]

2. EXPERIMENTAL SECTION

All organic thin films were grown under high-vacuum conditions by molecular-beam deposition from resistively heated Knudsen cells. SiO_2 substrates were cleaned by rinsing in ethanol and acetone. Atomically smooth graphite surfaces were prepared via exfoliation of HOPG substrates (ZYA quality, mosaic spread <0.4°) in air or using graphene-coated quartz substrates (Graphenea, Spain). The KCl(100) surfaces were prepared by cleaving slabs from a single crystal rod (Korth Kristalle) in air. After loading into the vacuum chamber, all substrates were heated at 500 K to remove residual contaminations and the incorporated water. Pentacene (PEN; Sigma-Aldrich) and perfluoropentacene (PFP; Kanto Denka Kogyo Co.) growth rates were monitored by a quartz crystal microbalance and films were processed at rates of about 6 Å min^{-1}. Complementary layers of 5,7,12,14-pentacenetetrone (P-TET, $C_{22}H_{10}O_4$; abcr GmbH) and *p*-sexiphenylene (*p*-6P, $C_{36}H_{26}$; TCI GmbH) were prepared using equivalent deposition conditions.

Thin films in upright orientations have been prepared by using oxidized silicon wafers as substrates,[44,46] while graphite and graphene samples have been used to prepare molecules in lying configurations[22,25,45,47] using the above-mentioned process parameters. To prevent effects from contamination, all samples were prepared without contact to air; i.e., the pure compound films as well as the films with small and large thickness of the top compound were prepared separately. The stacked films were prepared at room temperature to prevent molecular intermixture, which occurs at higher temperatures. In selected cases, the pure compound films have been prepared at 330 K to enhance the crystallite sizes.

The morphology of the films was characterized by AFM using an Agilent SPM 5500 system operated in tapping mode. MikroMasch cantilevers with a resonance frequency of about 325 kHz and a spring constant of 40 N m^{-1} were used. The crystalline structure of the samples was investigated by means of XRD with a Bruker D8 Discovery diffractometer using Cu Kα radiation.

NEXAFS measurements were performed at the HE-SGM dipole beamline of the synchrotron storage ring BESSY II in Berlin, providing linearly polarized light (polarization factor = 0.91) and an energy resolution at the C K-edge of about 300 meV. All NEXAFS spectra were recorded in partial electron yield mode using a channel-plate detector with a retarding field of −150 V. For calibration of the absolute energy scale, the photocurrent from a carbon-coated gold grid in the incident beam (absorption maximum = 284.9 eV) was recorded simultaneously. To determine the average molecular orientation relative to the sample surface, NEXAFS spectra were recorded at different angles of incidence (30°, 55°, 70°, and 90°), and the observed dichroism was analyzed after flux normalization and considering the transmission of the monochromator. Contributions from the substrate that overlap with the sample signature were subtracted to isolate the sample spectra, and the signal contributions of both compounds were separated by the appropriate subtraction of the pure compound spectra (details are given in the Supporting Information).

3. RESULTS AND DISCUSSION

A. Interface between the Template and Top Layer. The molecular orientation of the heterostructures at the interface between the template and templated top layer has been determined by analyzing the dichroism observed in NEXAFS spectroscopy measurements for samples with very thin top layers (d_{nom} = 2 nm). Because the characteristic NEXAFS signatures of PEN and PFP are sufficiently energy-separated, they can be well distinguished from another and thus allow an independent investigation of the molecular orientation of both compounds (for more information on the experimental setups and data processing, see the Supporting Information).

The corresponding data sets are presented in Figure 2. As shown in panel (a) for small amounts of PEN deposited on top

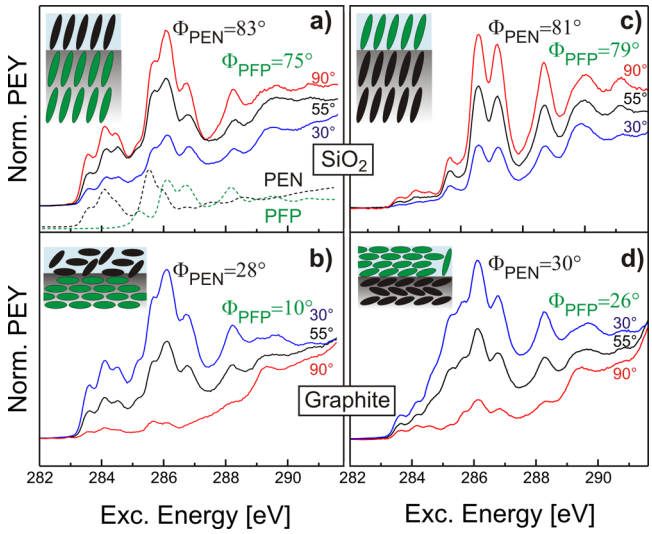

Figure 2. C 1s NEXAFS spectra of the initial growth (2 nm) of a second compound on the multilayer film (30 nm) of the first compound: PEN on PFP on (a) SiO_2, together with spectra of pure PEN (black dashed line) and PFP (green dashed line), and (b) graphite; PFP on PEN on (c) SiO_2 and (d) graphite with schemes of the molecular arrangements. Angles ϕ denote the determined molecular orientation of the individual compounds (angle between the molecular and surface planes).

of PFP templates with upright molecular orientation, the strongest absorption efficiency is found under normal incidence (θ = 90°, red curve), while rather weak absorption in the energy range between 282 and 288 eV occurs under gracing incidence (θ = 30°). Because the resonances at these energies correspond to excitations into unoccupied π^* orbitals, the transition dipole moments (TDM) of these resonances are known to be oriented normal to the molecular backbone.[49] Therefore, the molecular orientation in the top layers can be precisely determined.

As summarized in Table 1, this analysis reveals that indeed in the top layer the vertical orientation of the templating bottom layer is adopted. In the case of upright orientations of the molecules in the bottom layer, the molecular orientations are equal in the range of experimental error ($\Delta\phi \approx 5°$). The deposition of small amounts of PEN onto PFP in a lying orientation (ϕ_{PFP} = 10°) leads to an orientation of the PEN molecules of ϕ_{PEN} = 28°. Clearly, this value corresponds to molecules in a rather lying conformation. However, it is significantly higher than the value found for the PFP molecules in the bottom layer. This can be understood by considering the

DOI: 10.1021/acsami.5b07409
ACS Appl. Mater. Interfaces 2015, 7, 20485−20492

Table 1. Determined Effective Molecular Orientations from NEXAFS Dichroisms for Thin Template Top Layers Deposited on Differently Oriented Templating Bottom Layers

	PEN on PFP	PFP on PEN
upright	ϕ_{PEN} = 83° (top layer), ϕ_{PFP} = 75° (bottom layer)	ϕ_{PFP} = 79° (top layer), ϕ_{PEN} = 81° (bottom layer)
lying	ϕ_{PEN} = 28° (top layer), ϕ_{PFP} = 10° (bottom layer)	ϕ_{PFP} = 26° (top layer), ϕ_{PEN} = 30° (bottom layer)

packing motif of PEN in its crystalline arrangement. Because of the herringbone angle between both molecules of about 55°, the molecular backbones of the individual molecules cannot be perfectly parallel to one another. Instead, one molecule that adopts a horizontal backbone orientation always comes along with one molecule that has a significantly tilted short axis [cf. visualization of the $(1\bar{2}\bar{1})_{PEN}$ orientation presented in section B]. Because the orientations derived by NEXAFS are determined by incoherent contributions of all molecules, the lowest possible TDM orientation of PEN amounts to 28°.[22] Therefore, the determined orientation corresponds to a lying orientation of the molecules such that the long axis of the molecules is parallel to the surface but some molecules exhibit tilts of their short axis. We note that the derived value of 28° does not allow one to directly differentiate between an arrangement where all molecules are tilted by this value and a balanced coexistence between perfectly flat molecules (long and short axes of the molecules parallel to the surface) and molecules tilted by about 55°. The sketched arrangement in Figure 2 therefore corresponds to the structure motif that has been deduced from the XRD measurements (presented in the next section), showing that the first mentioned scenario is correct, which is perfectly compatible with the determined orientation of the PEN molecules.

Upon deposition of PFP on top of PEN, a similar situation is found. The PEN molecules adopt a lying orientation with a TDM orientation equivalent to that found on top of PFP (ϕ_{PEN} = 30°). The geometry of the PFP molecules in the top layer is again very similar to that of the PEN molecules in the bottom layer and amounts to ϕ_{PFP} = 26°. The higher value compared to PFP growth on pristine graphite (ϕ_{PFP} = 10°) results from the higher roughness of the PEN template compared to pristine graphite surfaces. This results in slight misorientations at the interface, which are healed out in thicker layers (see section B), possibly accompanied by individual uprightly oriented molecules nucleating at surface defects (cf. the inset in Figure 2d).[25] Taking this into account, the derived orientation of the PFP molecules clearly proves that the discussed templating effect is also observed for this case. Furthermore, it should be noted that this TDM orientation cannot be explained by any configuration in the PFP bulk structure. On the basis of arguments similar to those for the case of PEN molecules, the lowest observable TDM orientation for PFP in its bulk structure is 45° (in this case, higher than that for PEN because of the perpendicular herringbone angle in the PFP unit cell). Clearly, the present value is not compatible with the PFP bulk structure, hence indicating that in this case the molecules have crystallized in a different polymorph with a less pronounced herringbone angle. The observation of this π-stacked PFP polymorph will be discussed in detail in the next section.

B. Top Layers with Increased Thickness. Morphological analyses of heterostructures with higher amounts of the top compound (typically 30 nm nominal thickness) show that the morphologies observed at the interfaces persist well into the thicker layers, indicating that also the orientations are equivalent (a complete set of AFM micrographs is presented in the Supporting Information). Furthermore, morphological analyses allow one to derive that the top layer covers the bottom layer rather homogeneously, thus indicating efficient wetting, as exemplarily presented in Figure 3 for hetero-

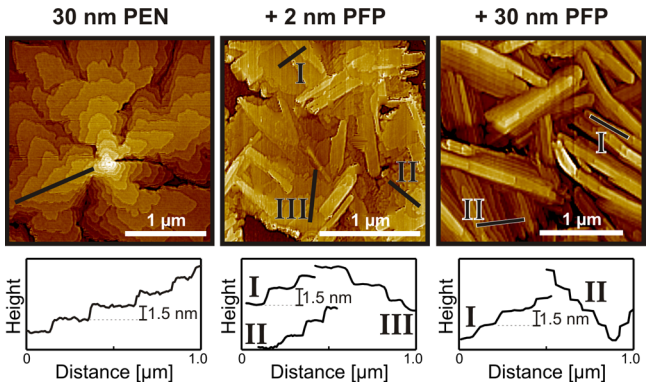

Figure 3. AFM micrographs of (a) a PEN template layer (30 nm) in an upright molecular orientation (on SiO_2) and templated heterostructures with (b) 2 nm PFP and (c) 30 nm PFP, showing that the morphology at the interface is similar to that in larger thicknesses. Furthermore, efficient wetting of the PFP film on the PEN template can be clearly observed.

structures where PFP has been deposited on top of PEN in an upright molecular orientation. In this case, also monomolecular steps can be observed, which correspond to upright molecular orientations in both layers, suggesting that the upright orientation of the template is indeed adopted in the templated layer.

The sufficient scattering intensity of the extended top layers also allows for their analysis by means of XRD, enabling the precise identification of the crystalline phases. These measurements are summarized in Figure 4. For both heterostructures

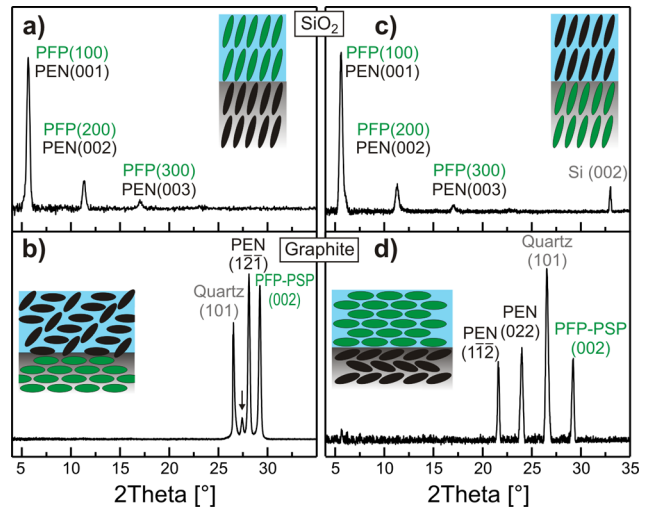

Figure 4. X-ray diffractograms of PEN/PFP stacks with nominal thickness of 30 nm in the top and bottom layers: PEN on PFP on (a) SiO_2 and (b) graphite; PFP on PEN on (c) SiO_2 and (d) graphite. Schemes of the molecular arrangements are shown in the respective insets.

DOI: 10.1021/acsami.5b07409
ACS Appl. Mater. Interfaces 2015, 7, 20485−20492

with upright molecular orientation in the bottom compound layer, only the $(n00)_{PFP}$ and $(00n)_{PEN}$ reflexes are observed, which correspond to upright orientations.[50] Therefore, it can be concluded that the upright orientation of the bottom layer is perfectly transferred into the top layer also for increased thicknesses. In the case of lying PFP molecules as templates, three peaks in addition to the substrate signal are observed (cf. Figure 4c): a peak at $2\theta = 29.4°$ resulting from PFP molecules in a lying, parallel configuration [(002) orientation in the π-stacked polymorph (PSP, details below)], the $(1\bar{2}\bar{1})_{PEN}$ peak,[51] and an additional peak at $2\theta = 27.5°$ that cannot be attributed to either PEN or PFP. Previous studies have shown that PEN and PFP are capable of forming stoichiometric intermixed crystals with an alternating arrangement of both opponent molecules.[52,53] Therefore, this unacquainted signal is attributed to the formation of regions with molecular intermixture at the interface. Indeed, in a recent study, it has been shown that such an intermixture can occur not only upon the simultaneous evaporation of both compounds but also upon subsequent deposition.[54] Because this intermixture is thermally activated, all stacks have been prepared at room temperature to minimize this intermixture and no indications of an intermixture have been found for the other samples. In the $(1\bar{2}\bar{1})$ plane, both PEN molecules in the unit cell adopt configurations with their long axis oriented parallel to the surface but different tilts of their short axis: while one molecule lies nearly perfectly horizontal on the surface, the other one is inclined with its short axis by about 55° (cf. the scheme in Figure 4b and visualization of the packing motif in Figure 5). Nevertheless, again it can be clearly stated that the lying orientation of the PFP molecules in the bottom layer is inherited in the PEN molecules in the top layer.

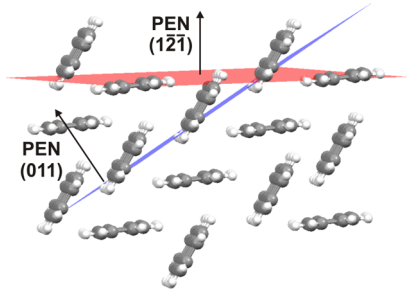

Figure 5. Sketch of the molecular arrangement of PEN adopted in the $(1\bar{2}\bar{1})$ and (011) planes. Despite slight tilts of the molecular backbone, all molecules are aligned with their long axis parallel to the planes shown.

The diffraction patterns acquired for PFP multilayer films prepared on top of PEN templates in a lying molecular conformation again reveal three thin-film related peaks: $(1\bar{1}2)_{PEN}$ and $(022)_{PEN}$ peaks as well as the PFP $(002)_{PSP}$ peak. The observation of the two first peaks, which again correspond to lying orientations of the PEN molecules with slight tilts of the short axis, is in good agreement with previous studies on the growth of unitary PEN films on graphite and graphene surfaces.[22,47] As mentioned before, the PFP-related peak does not result from a lattice plane in the original PFP bulk crystal structure but instead is a fingerprint of a distinctly different polymorph, where the PFP molecules adopt a coplanar configuration without a herringbone angle (cf. Figure 6a). This π-stacked polymorph has so far only been observed

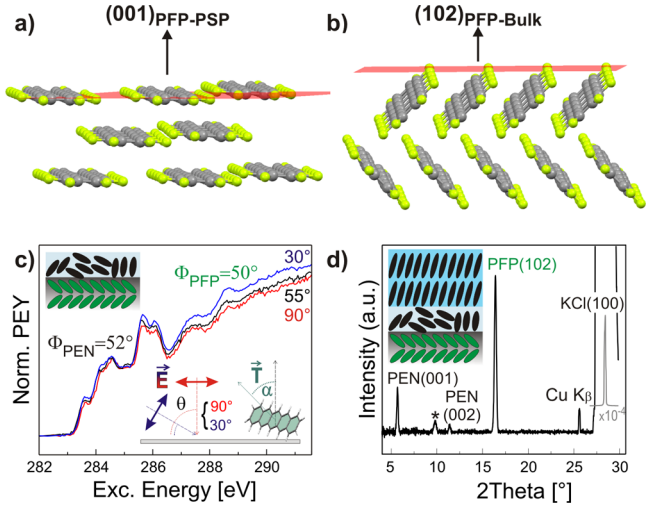

Figure 6. Investigations of heterostructures with lying PFP in a herringbone arrangement on KCl(100) substrates. (a) Scheme of the molecular arrangement of π-stacked PFP, as observed on graphite; (b) herringbone-lying arrangement of PFP on KCl(100); (c) NEXAFS dichroism; (d) X-ray diffractogram of the heterostructures with corresponding molecular schemes. The asterisk denotes contributions of $\lambda/3$ content in the X-ray beam.

for PFP thin films grown on graphite or on Ag(111) and has been attributed to lattice matching respectively strong interaction with the substrate.[45,55] Its occurrence also in heteroorganic stacks with pentacene is therefore somewhat unexpected. This is especially true because the mutual interaction between PFP and PEN is considerably weaker than that with a metal substrate and the surface of the template exhibits significant nanoroughness because of the slight molecular tilt angle of 28° of the bottom PEN molecules (cf. Figure 5), which was expected to prevent efficient lattice matching at the interface. In all cases of templates with a lying orientation in the bottom layer compound, no diffraction peaks related to upright orientations in the top-layer compounds are observed, thus underlining the stability of this concept.

To further investigate the stability of the heterostructures over time and upon postheating, additional experiments have been conducted to address this issue. For that purpose, the multilayer samples have been characterized in an equal manner after 6 months of aging under environmental conditions and furthermore after postheating to temperatures of 373 K. Because no indications for structural transitions have been found, we conclude that the present molecular heterostructures are stable against aging and heat-induced structural changes (corresponding data are presented in the Supporting Information).

C. Influence of Molecular Polymorphism. In addition, we have addressed the influence of molecular polymorphism on the concept of orientation inheritance. To this end, also heterostacks of PEN and PFP have been prepared on KCl (100) surfaces. There, the PFP molecules again adsorb with their long axis parallel to the surface like on graphite. However, the molecules crystallize in the bulk herringbone polymorph in the $(102)_{PFP}$ orientation instead of the coplanar π-stacked polymorph as on graphite.[23] The most important difference between both geometries is the perfectly flat arrangement of the PFP molecules on graphite surfaces compared to the significantly tilted molecules (with their short axis) in thin films on KCl, yielding an angle of 45° between their short axis and

DOI: 10.1021/acsami.5b07409
ACS Appl. Mater. Interfaces 2015, 7, 20485−20492

the surface (cf. Figure 6a,b). This enables one to study the resulting orientation of PEN layers on top of PFP thin films in a lying orientation but different polymorphs. Indeed, the orientation of the on-top pentacene layer is strongly different in this case. As derived from the NEXAFS spectra presented in Figure 6c, the effective TDM orientation of PEN molecules at the interface amounts to 52°, which corresponds to either molecules in a disordered fashion or the coexistence of domains with upright and lying molecular orientations. In thicker top layers, PEN crystallizes in an upright orientation, as reflected by the exclusive appearance of the $(00n)_{PEN}$ diffraction peaks in the XRD patterns presented in Figure 6d,[56] which resembles the situation of PEN growth on polycrystalline gold.[57] Clearly, this situation is strongly different from the adsorption of pentacene on π-stacked PFP on graphite, where also the pentacene molecules adopt a lying orientation at the interface as well as in thicker layers.

D. Inheriting Molecular Orientation for Other Organic Materials. So far, the concept of inheriting molecular orientations has been discussed for the combination of PEN and PFP. To find out about the applicability of this concept also for other materials, two additional material combinations have been studied. Commonly an upright molecular orientation is found in thin films grown on weakly interacting substrates like SiO_2 because the surface free energy is lowest in such configurations and the substrate−adsorbate interaction is too weak to influence the molecular orientation.[13,44,46] Therefore, the inspection of stacks with a lying molecular orientation in the bottom layer appears to be the more interesting case to investigate the effect of structural inheritance. To that purpose, bottom layers with PFP molecules in a lying configuration, as prepared on graphite surfaces, are used on which multilayer films of P-TET and *p*-6P have been prepared. These two compounds appear to be rather interesting because they represent different levels of similarity compared to PFP. In the previously considered heterostructures of PEN and PFP, both compounds are structurally similar and furthermore exhibit strong quadrupolar interaction because of the inverted charge-carrier distribution resulting from the fluorinated rim of PFP. Clearly, P-TET is again rather similar from a structural point of view because the molecular backbone is nearly equal to that of PEN (cf. the scheme of the molecule in Figure 7a), but the quadrupolar interaction between both compounds is clearly reduced compared to the combination PEN/PFP. *p*-6P, finally, is an OSC that features a structure distinctly different from that of PEN and its derivatives (cf. Figure 7b).

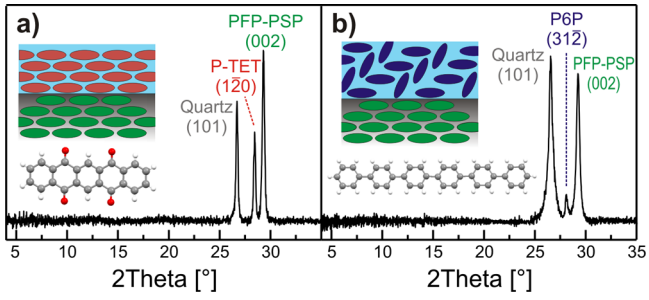

Figure 7. X-ray diffractograms of (a) P-TET, (b) *p*-6P multilayer films deposited onto PFP templates with molecules in a lying orientation (prepared on graphite substrates). The exclusive observation of the $(1\bar{2}0)_{P\text{-}TET}$ and $(31\bar{2})_{p\text{-}6P}$ peaks shows that the lying orientation of the PFP bottom layer is adopted in the templated top layer, as depicted by the schematics of the molecular arrangements.

As presented in Figure 7, the final structures of multilayer films in these combinations have been analyzed by means of XRD analyses. For both combinations, only one additional peak besides the substrate peak and the PFP-related signal is observed. In the case of P-TET, a peak at $2\theta = 28.3°$ emerges that corresponds to the $(1\bar{2}0)_{P\text{-}TET}$ orientation. In this crystalline arrangement, the molecules adopt a perfectly lying orientation that is comparable to that of the PFP molecules (cf. the inset in Figure 7a) and detailed visualization in the Supporting Information). Such a coplanar orientation can be adopted by the P-TET molecules—in contrast to PEN molecules, as discussed before—because the P-TET molecules do not crystallize in a herringbone arrangement but in a coplanar configuration as a result of the electrostatic coupling between the individual molecules.[58]

For the *p*-6P/PFP stacks, finally, only one *p*-6P-related signal at $2\theta = 28.2°$ is observed. This value represents the $(31\bar{2})_{P6P}$ orientation, which again corresponds to molecules oriented with their long axis parallel to the surface (i.e., lying configuration). Because of the herringbone packing in the crystal structure, some molecules feature tilts of their short axis, like in the case of pentacene on PFP templates with a lying molecular orientation.

In previous studies by Koller et al. and Oehzelt et al., it has been shown that the molecular orientation of *p*-6P molecules can also be transferred to top layers of 6T and vice versa,[33,34] and similar observations were made for the combination of CuPc and PTCDA by Chen et al.[35] Therefore, a comparison of their results with our reports on structural inheritance for the case of structurally similar (PEN and PFP) as well as structurally inequivalent molecules (PFP, P-TET, and *p*-6P) indicates that structural inheritance seems to be a rather general concept to gain structural control in organic heterostructures.

4. CONCLUSION

In summary, we have demonstrated that ordered molecular films can serve as templates for heteromolecular growth and thus enable structural control over subsequently grown heterolayers. As summarized in Figure 8, for the case of PEN/PFP heterostructures, the initial orientation of the template layer is passed on to the templated top layer of the antipodal molecule both at the interface with the template and in thicker layers of the templated top layer. This proves the stability of this concept, especially compared to substrate-mediated growth utilizing inorganic, e.g., metal surfaces, where the initial orientation at the interface does not reside in consecutive molecular layers. Moreover, we note that in single-crystal-mediated growth of unitary thin films a high

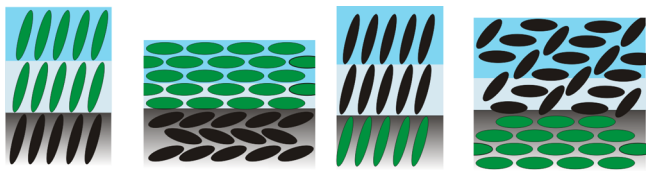

Figure 8. Summary of obtained PEN/PFP heterostructures using the concept of templated templates. In all cases the molecular orientation of the bottom layer is also adopted in the top layer (color code like in Figure 1).

DOI: 10.1021/acsami.5b07409
ACS Appl. Mater. Interfaces 2015, 7, 20485−20492

susceptibility of the final molecular orientation on the coherence and long-range smoothness of the substrate has been reported.[22,25,59] By contrast, the presently studied organic multilayer templates render an inheritance of the template orientation possible despite the comparably high roughness of the templates. Interestingly, the template orientation is maintained in a film thickness of 30 nm, thus providing an interesting route to facilitate complex heterostructures with the desired molecular orientation.

The present study indicates that molecular recognition is of key importance in controlling the molecular orientation in seed layers, which are decisive for the molecular orientation and crystalline assembly upon subsequent film growth. This approach appears to be very useful because it enables model studies with well-defined molecular interfaces. Such systems are of importance for various fields ranging from biological interfaces aimed at understanding molecular recognition processes[60,61] to organic photovoltaics enabling microscopic studies of charge-transfer processes at acceptor/donor interfaces with specific molecular orientation.

■ ASSOCIATED CONTENT

Supporting Information

The Supporting Information is available free of charge on the ACS Publications website at DOI: 10.1021/acsami.5b07409.

Details on sample preparation and experimental characterization, full data sets of AFM micrographs, NEXAFS spectra, XRD diffractograms, and details on data analysis (PDF)

■ AUTHOR INFORMATION

Corresponding Author

*E-mail: tobias.breuer@physik.uni-marburg.de.

Notes

The authors declare no competing financial interest.

■ ACKNOWLEDGMENTS

We acknowledge support by the Deutsche Forschungsgemeinschaft (Grant SFB 1083, TP A2) and the Helmholtz-Zentrum Berlin (electron storage ring BESSY II) for provision of synchrotron radiation at beamline HE-SGM.

■ REFERENCES

(1) Richter, J.; Mertig, M.; Pompe, W.; Mönch, I.; Schackert, H. Construction of Highly Conductive Nanowires on a DNA Template. *Appl. Phys. Lett.* **2001**, *78*, 536−538.

(2) Gothelf, K.; LaBean, T. DNA-Programmed Assembly of Nanostructures. *Org. Biomol. Chem.* **2005**, *3*, 4023−4037.

(3) Mahmoudi, M.; Bonakdar, S.; Shokrgozar, M.; Aghaverdi, H.; Hartmann, R.; Pick, A.; Witte, G.; Parak, W. Cell-Imprinted Substrates Direct the Fate of Stem Cells. *ACS Nano* **2013**, *7*, 8379−8384.

(4) Mann, S. Molecular Tectonics in Biomineralization and Biomimetic Materials Chemistry. *Nature* **1993**, *365*, 499−505.

(5) Sarikaya, M.; Tamerler, C.; Jen, A. K.-Y.; Schulten, K.; Baneyx, F. Molecular Biomimetics: Nanotechnology through Biology. *Nat. Mater.* **2003**, *2*, 577−585.

(6) Falini, G.; Albeck, S.; Weiner, S.; Addadi, L. Control of Aragonite or Calcite Polymorphism by Mollusk Shell Macromolecules. *Science* **1996**, *271*, 67−69.

(7) Love, J. C.; Estroff, L. A.; Kriebel, J. K.; Nuzzo, R. G.; Whitesides, G. M. Self-Assembled Monolayers of Thiolates on Metals as a Form of Nanotechnology. *Chem. Rev.* **2005**, *105*, 1103−1169.

(8) Schreiber, F. Structure and Growth of Self-Assembling Monolayers. *Prog. Surf. Sci.* **2000**, *65*, 151−257.

(9) Barth, J.; Costantini, G.; Kern, K. Engineering Atomic and Molecular Nanostructures at Surfaces. *Nature* **2005**, *437*, 671−679.

(10) Barth, J. Molecular Architectonic on Metal Surfaces. *Annu. Rev. Phys. Chem.* **2007**, *58*, 375−407.

(11) Barth, J.; Weckesser, J.; Lin, N.; Dmitriev, A.; Kern, K. Supramolecular Architectures and Nanostructures at Metal Surfaces. *Appl. Phys. A: Mater. Sci. Process.* **2003**, *76*, 645−652.

(12) Barlow, S.; Raval, R. Complex Organic Molecules at Metal Surfaces: Bonding, Organisation and Chirality. *Surf. Sci. Rep.* **2003**, *50*, 201−341.

(13) Ambrosch-Draxl, C.; Nabok, D.; Puschnig, P.; Meisenbichler, C. The Role of Polymorphism in Organic Thin Films: Oligoacenes Investigated from First Principles. *New J. Phys.* **2009**, *11*, 125010.

(14) Zhou, H.-C.; Long, J.; Yaghi, O. Introduction to Metal−Organic Frameworks. *Chem. Rev.* **2012**, *112*, 673−674.

(15) Liu, B.; Ma, M.; Zacher, D.; Bétard, A.; Yusenko, K.; Metzler-Nolte, N.; Wöll, C.; Fischer, A. A. Chemistry of SURMOFs: Layer-Selective Installation of Functional Groups and Post-synthetic Covalent Modification Probed by Fluorescence Microscopy. *J. Am. Chem. Soc.* **2011**, *133*, 1734−1737.

(16) Shekhah, O.; Wang, H.; Paradinas, M.; Ocal, C.; Schüpbach, B.; Terfort, A.; Zacher, D.; Fischer, R. A.; Wöll, C. Controlling Interpenetration in Metal−Organic Frameworks by Liquid-phase Epitaxy. *Nat. Mater.* **2009**, *8*, 481−484.

(17) Hermes, S.; Schröder, F.; Chelmowski, R.; Wöll, C.; Fischer, R. Selective Nucleation and Growth of Metal−Organic Open Framework Thin Films on Patterned COOH/CF3-Terminated Self-Assembled Monolayers on Au(111). *J. Am. Chem. Soc.* **2005**, *127*, 13744−13745.

(18) Sai, N.; Tiago, M. L.; Chelikowsky, J. R.; Reboredo, F. A. Optical Spectra and Exchange-Correlation Effects in Molecular Crystals. *Phys. Rev. B: Condens. Matter Mater. Phys.* **2008**, *77*, 161306.

(19) Albrecht, A. C. Polarizations and Assignments of Transitions: The Method of Photoselection. *J. Mol. Spectrosc.* **1961**, *6*, 84−108.

(20) Valeur, B.; Berberan-Santos, M. N. *Molecular Fluorescence*; Wiley-VCH: Heidelberg, Germany, 2012.

(21) Silinsh, E. A.; Čápek, V. *Organic Molecular Crystals*; AIP Press: New York, 1994.

(22) Götzen, J.; Käfer, D.; Wöll, C.; Witte, G. Growth and Structure of Pentacene Films on Graphite: Weak Adhesion as a Key for Epitaxial Film Growth. *Phys. Rev. B: Condens. Matter Mater. Phys.* **2010**, *81*, 085440.

(23) Breuer, T.; Witte, G. Epitaxial Growth of Perfluoropentacene Films with Predefined Molecular Orientation: A Route for Single-crystal Optical Studies. *Phys. Rev. B: Condens. Matter Mater. Phys.* **2011**, *83*, 155428.

(24) Kiyomura, T.; Nemoto, T.; Yoshida, K.; Minari, T.; Kurata, H.; Isoda, S. Epitaxial Growth of Pentacene Thin-film Phase on Alkali Halides. *Thin Solid Films* **2006**, *515*, 810−813.

(25) Breuer, T.; Salzmann, I.; Götzen, J.; Oehzelt, M.; Morherr, A.; Koch, N.; Witte, G. Interrelation between Substrate Roughness and Thin-film Structure of Functionalized Acenes on Graphite. *Cryst. Growth Des.* **2011**, *11*, 4996−5001.

(26) Götzen, J.; Lukas, S.; Birkner, A.; Witte, G. Absence of Template Induced Ordering in Organic Multilayers: The Growth of Pentacene on a Cu(221) Vicinal Surface. *Surf. Sci.* **2011**, *605*, 577−581.

(27) Peisert, H.; Biswas, I.; Zhang, L.; Knupfer, M.; Hanack, M.; Dini, D.; Cook, M.; Chambrier, I.; Schmidt, T.; Batchelor, D.; Chassé, T. Orientation of Substituted Phthalocyanines on Polycrystalline Gold: Distinguishing between the First Layers and Thin Films. *Chem. Phys. Lett.* **2005**, *403*, 1−6.

(28) Witte, G.; Wöll, C. Growth of Aromatic Molecules on Solid Substrates for Applications in Organic Electronics. *J. Mater. Res.* **2004**, *19*, 1889−1916.

(29) Yi, Y.; Coropceanu, V.; Bredas, J.-L. Exciton-Dissociation and Charge-Recombination Processes in Pentacene/C60 Solar Cells: Theoretical Insight into the Impact of Interface Geometry. *J. Am. Chem. Soc.* **2009**, *131*, 15777−15783.

DOI: 10.1021/acsami.5b07409
ACS Appl. Mater. Interfaces 2015, 7, 20485−20492

(30) Lunt, R. R.; Benziger, J. B.; Forrest, S. R. Relationship between Crystalline Order and Exciton Diffusion Length in Molecular Organic Semiconductors. *Adv. Mater.* **2010**, *22*, 1233−136.
(31) Bouthinon, B.; Clerc, R.; Vaillant, J.; Verilhac, J.-M.; Faure-Vincent, J.; Djurado, D.; Ionica, I.; Man, G.; Gras, A.; Pananakakis, G.; Gwoziecki, R.; Kahn, A. Impact of Blend Morphology on Interface State Recombination in Bulk Heterojunction Organic Solar Cells. *Adv. Funct. Mater.* **2015**, *25*, 1090−1101.
(32) Zhugayevych, A.; Tretiak, S. Theoretical Description of Structural and Electronic Properties of Organic Photovoltaic Materials. *Annu. Rev. Phys. Chem.* **2015**, *66*, 305−330.
(33) Koller, G.; Berkebile, S.; Krenn, J.; Netzer, F.; Oehzelt, M.; Haber, T.; Resel, R.; Ramsey, M. Heteroepitaxy of Organic-Organic Nanostructures. *Nano Lett.* **2006**, *6*, 1207−1212.
(34) Oehzelt, M.; Koller, G.; Ivanco, J.; Berkebile, S.; Haber, T.; Resel, R.; Netzer, F. P.; Ramsey, M. G. Organic Heteroepitaxy: p-Sexiphenyl on Uniaxially Oriented α-Sexithiophene. *Adv. Mater.* **2006**, *18*, 2466−2470.
(35) Chen, W.; Huang, H.; Chen, S.; Chen, L.; Zhang, H. L.; Gao, X. Y.; Wee, A. T. S. Molecular Orientation of 3,4,9,10-Perylene-Tetracarboxylic-Dianhydride Thin Films at Organic Heterojunction Interfaces. *Appl. Phys. Lett.* **2007**, *91*, 114102.
(36) Chen, W.; Qi, D.-C.; Huang, H.; Gao, X.; Wee, A. T. S. Organic−Organic Heterojunction Interfaces: Effect of Molecular Orientation. *Adv. Funct. Mater.* **2011**, *21*, 410−424.
(37) Hinderhofer, A.; Schreiber, F. Organic−Organic Heterostructures: Concepts and Applications. *ChemPhysChem* **2012**, *13*, 628−643.
(38) Hinderhofer, A.; Gerlach, A.; Kowarik, S.; Zontone, F.; Krug, J.; Schreiber, F. Smoothing and Coherent Structure Formation in Organic-Organic Heterostructure Growth. *Europhys. Lett.* **2010**, *91*, 56002.
(39) Duhm, S.; Salzmann, I.; Heimel, G.; Oehzelt, M.; Haase, A.; Johnson, R. L.; Rabe, J. P.; Koch, N. Controlling Energy Level Offsets in Organic/Organic Heterostructures using Intramolecular Polar Bonds. *Appl. Phys. Lett.* **2009**, *94*, 033304.
(40) Gordan, I.; Sakurai, T.; Friedrich, M.; Akimoto, K.; Zahn, D. Ellipsometric Study of an Organic Template Effect: H2Pc/PTCDA. *Org. Electron.* **2006**, *7*, 521−527.
(41) Schmitz-Hübsch, T.; Sellam, F.; Staub, R.; Törker, M.; Fritz, T.; Kübel, C.; Müllen, K.; Leo, K. Direct Observation of Organic−Organic Heteroepitaxy: Perylene-tetracarboxylic-Dianhydride on Hexa-peri-benzocoronene on Highly Ordered Pyrolytic Graphite. *Surf. Sci.* **2000**, *445*, 358−367.
(42) Stadtmüller, B.; Sueyoshi, T.; Kichin, G.; Kröger, I.; Soubatch, S.; Temirov, R.; Tautz, F.; Kumpf, C. Commensurate Registry and Chemisorption at a Hetero-organic Interface. *Phys. Rev. Lett.* **2012**, *108*, 106103.
(43) Sakamoto, Y.; Suzuki, T.; Kobayashi, M.; Gao, Y.; Fukai, Y.; Inoue, Y.; Sato, F.; Tokito, S. Perfluoropentacene: High-Performance p−n Junctions and Complementary Circuits with Pentacene. *J. Am. Chem. Soc.* **2004**, *126*, 8138−8140.
(44) Bouchoms, I.; Schoonveld, W.; Vrijmoeth, J.; Klapwijk, T. Morphology Identification of the Thin Film Phases of Vacuum Evaporated Pentacene on SIO2 Substrates. *Synth. Met.* **1999**, *104*, 175−178.
(45) Salzmann, I.; Moser, A.; Oehzelt, M.; Breuer, T.; Feng, X.; Juang, Z.-Y.; Nabok, D.; Della Valle, R. D.; Duhm, S.; Heimel, G.; Brillante, A.; Venuti, E.; Bilotti, I.; Christodoulou, C.; Frisch, J.; Puschnig, P.; Draxl, C.; Witte, G.; Müllen, K.; Koch, N. Epitaxial Growth of π-stacked Perfluoropentacene on Graphene-coated Quartz. *ACS Nano* **2012**, *6*, 10874−10883.
(46) Kowarik, S.; Gerlach, A.; Hinderhofer, A.; Milita, S.; Borgatti, F.; Zontone, F.; Suzuki, T.; Biscarini, F.; Schreiber, F. Structure, Morphology, and Growth Dynamics of Perfluoro-pentacene Thin Films. *Phys. Status Solidi RRL* **2008**, *2*, 120−122.
(47) Lee, W. H.; Park, J.; Sim, S. H.; Lim, S.; Kim, K. S.; Hong, B. H.; Cho, K. Surface-Directed Molecular Assembly of Pentacene on Monolayer Graphene for High-Performance Organic Transistors. *J. Am. Chem. Soc.* **2011**, *133*, 4447−4454.
(48) Breuer, T.; Klues, M.; Witte, G. Characterization of Orientational Order in π-conjugated Molecular Thin Films by NEXAFS. *J. Electron Spectrosc. Relat. Phenom.* **2015**, DOI: 10.1016/j.elspec.2015.07.011.
(49) Ågren, H.; Vahtras, O.; Carravetta, V. Near-edge Core Photoabsorption in Polyacenes: Model Molecules for Graphite. *Chem. Phys.* **1995**, *196*, 47−58.
(50) Because of their nearly identical vertical spacing, the $(n00)_{PFP}$ ($d_{(100)PFP}$ = 15.5 Å) and $(00n)_{PEN,TF}$ ($d_{(001)PEN,TF}$ = 15.4 Å) related peaks cannot be directly separated in the specular X-ray diffractograms. Nevertheless, the existence of both crystalline phases could be precisely verified by comparing the X-ray diffractograms of the pure compound templates with those of the heterostructures because the additional templated film in the heterostructures results in significantly enhanced peak intensities compared to those of the pure compound films.
(51) Pentacene is known to form crystalline thin films in different molecular polymorphs with slightly different lattice parameters. The observed diffraction peaks in upright orientation $[(00n)_{PEN}]$ correspond to the thin-film phase, while the crystalline phases with a lying molecular orientation in each case can be assigned to the Siegrist phase (further information is given in the Supporting Information).
(52) Salzmann, I.; Duhm, S.; Heimel, G.; Rabe, J. P.; Koch, N.; Oehzelt, M.; Sakamoto, Y.; Suzuki, T. Structural Order in Perfluoropentacene Thin Films and Heterostructures with Pentacene. *Langmuir* **2008**, *24*, 7294−7298.
(53) Hinderhofer, A.; Frank, C.; Hosokai, T.; Resta, A.; Gerlach, A.; Schreiber, F. Structure and Morphology of Coevaporated Pentacene-perfluoropentacene Thin Films. *J. Chem. Phys.* **2011**, *134*, 104702.
(54) Breuer, T.; Witte, G. Thermally Activated Intermixture in Pentacene-perfluoropentacene Heterostructures. *J. Chem. Phys.* **2013**, *138*, 114901.
(55) Duhm, S.; Hosoumi, S.; Salzmann, I.; Gerlach, A.; Oehzelt, M.; Wedl, B.; Lee, T.-L.; Schreiber, F.; Koch, N.; Ueno, N.; Kera, S. Influence of Intramolecular Polar Bonds on Interface Energetics in Perfluoro-pentacene on Ag (111). *Phys. Rev. B: Condens. Matter Mater. Phys.* **2010**, *81*, 045418.
(56) Theoretically possible PEN peaks that are superimposed by the KCl (002) substrate signal can be safely ruled out because measurements with an intentional slight sample tilt, allowing us to fade out the substrate signal, have not revealed any peaks in that range.
(57) Käfer, D.; Ruppel, L.; Witte, G. Growth of Pentacene on Clean and Modified Gold Surfaces. *Phys. Rev. B: Condens. Matter Mater. Phys.* **2007**, *75*, 085309.
(58) Käfer, D.; El Helou, M.; Gemel, C.; Witte, G. Packing of Planar Organic Molecules: Interplay of van der Waals and Electrostatic Interaction. *Cryst. Growth Des.* **2008**, *8*, 3053−3057.
(59) McAfee, T.; Gann, E.; Guan, T.; Stuart, S.; Rowe, J.; Dougherty, D.; Ade, H. Toward Single-Crystal Hybrid-Carbon Electronics: Impact of Graphene Substrate Defect Density on Copper Phthalocyanine Film Growth. *Cryst. Growth Des.* **2014**, *14*, 4394−4401.
(60) Makrodimitris, K.; Masica, D. L.; Kim, E. T.; Gray, J. J. Structure Prediction of Protein−Solid Surface Interactions Reveals a Molecular Recognition Motif of Statherin for Hydroxyapatite. *J. Am. Chem. Soc.* **2007**, *129*, 13713−13722.
(61) Haino, T.; Matsumoto, Y.; Fukazawa, Y. Supramolecular Nano Networks Formed by Molecular-Recognition-Directed Self-Assembly of Ditopic Calix[5]arene and Dumbbell [60]Fullerene. *J. Am. Chem. Soc.* **2005**, *127*, 8936−8937.

DOI: 10.1021/acsami.5b07409
ACS Appl. Mater. Interfaces 2015, 7, 20485−20492